

16-QAM Photonic Vector Modulator for Gigabit Wireless Links

Autor: Rakesh Sambaraju

Director1: Juan Luis Corral

Resumen — Esta Tesina se centra en el uso de técnicas fotónicas aplicadas en los enlaces inalámbricos de alta capacidad en el rango de frecuencias de ondas milimétricas. En concreto, se ha propuesto una nueva técnica llamada modulación vectorial fotónica y se ha estudiado y demostrado experimentalmente la generación de modulación avanzada 16-QAM hasta una capacidad de 10 Gb/s en el rango de frecuencias de ondas milimétricas. Asimismo, se han propuesto y demostrado experimentalmente varias arquitecturas basadas en ciertos dispositivos ópticos para la generación de enlaces inalámbricos de alta capacidad con modulación 16-QAM. Las prestaciones de estas arquitecturas se han evaluado numéricamente.

Abstract — In this report the use of photonic techniques in the application of high capacity wireless links in the millimeter wave frequency range is addressed. A novel technique called the photonic vector modulation has been proposed, and generation of advanced modulation like 16-QAM upto a capacity of 10 Gb/s in the millimeter wave frequency has been studied and experimentally demonstrated. Several architectures based on certain optical devices, for the generation of such high capacity wireless links with 16-QAM modulation have been proposed and experimentally demonstrated. The performance of these architectures has been numerically evaluated.

Autor: Sambaraju R. ..., email: rsambaraju@ntc.upv.es

Director 1: Arroyo ..., email: arroyo@dcom.upv.es

Fecha de entrega: 30-02-07

ÍNDICE

I. Introduction	3
II. Working Principle	5
II.1. Mathematical Model.....	6
III. Experimental Demonstrations	8
III.1. Architecture 1: Direct Modulation Based PVM.....	8
III.1. Architecture 2: DD-MZM Based PVM.....	10
IV. 10 Gb/s 16-QAM Signal Generation	12
IV.1. Experimental Setup.....	13
IV.2. Results.....	14
IV. Conclusions	15
Agradecimientos	16
Referencias	16
Anexos	17

I. Introduction

Optical communication systems have taken a monumental leap in the last 20 years in terms of the capacity provided by them. With the recent advances in technologies related to high speed opto-electronic devices, and advanced modulation formats, single channel capacities of upto 100 Gb/s [1-3] are in development for metro and core networks. The optical transmission systems are not only seeing an increasing in capacity due to advanced modulation formats by electrical time domain multiplexing (ETDM), but also with the recent developments in optical time division multiplexed (OTDM) systems, single channels of upto x Tb/s are also possible [4]. This huge demand in the metro-core segment can be attributed to a certain extent to the access network segment, where with the invention of fibre to the home (FTTH) concept and passive optical networks, bit rates of upto 10 Gb/s with the current standard 10GEPON [5] are not far away from reality. The access networks are also considering the next generation PONs (NG-PON), where speeds of 40 Gb/s or even 100 Gb/s [6, 7] are in investigation. Even though the optical access networks provide a cheap access solution, thanks to the efforts done in making cost-effective devices, there will still be a great section of population, especially in remote areas, greenfield residential areas, villages, etc, where the deployment of new fibre will be challenging both from technical and economic perspective.

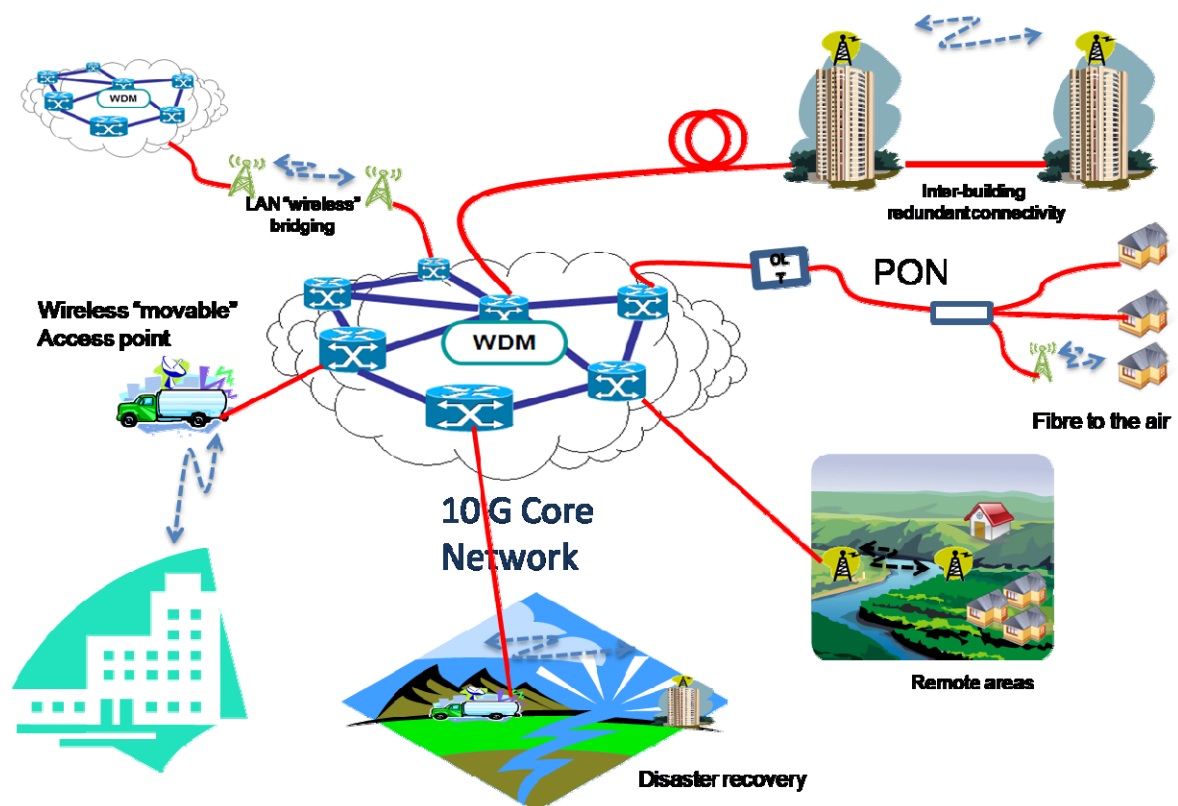


Fig.1. Artistic projection of the various application scenario of a gigabit wireless link.

Wireless access has classically been a solution for such bottle necks, and considering the advantages of wireless links in cost and ease, and time of deployment, wireless access of 10 Gb/s is

of great interest. Such high capacity wireless links not only provide the access solution, but also have several other applications like inter-building corporate LAN networks, disaster recovery links, redundancy links, and in battle field for realtime monitoring. Figure 1 shows a schematic of the several applications.

Band	Available Bandwidth (GHz)	EIRP	LICENSE/REGULATION
40 GHz	3.5 (40-43.5)	57 dBm	Yes (CEPT/FCC)
60 GHz	7 (57-64)	>40 dBm	No (CEPT/FCC)
70/80 GHz	10 (71-76/81-86)	55 dBW	Yes (CEPT/FCC)
>100 GHz	unlimited	N.A	N.A

Tabla 1: Unidades par alas propiedades magnéticas

Currently for providing gigabit connectivity wirelessly, the millimeter wave frequency bands like 40 GHz, 60 GHz, and 70/80 GHz offer a few GHz of bandwidth, which in combination with high spectral efficient modulation formats, 10 Gb/s links are possible. Table 1 summarises the millimeter wave bands and the available bandwidth. Making broadband devices with electric technology at these frequencies is very challenging and results in timing jitter, and group delay problems. Photonics and radio over fiber techniques [8, 9] offers a great solution to these high capacity wireless links, considering the various advantages of optical technologies like huge bandwidth, scalability, fiber transmission etc. Several research efforts on generation of high capacity wireless links using photonic techniques are underway [10-16]. Most of these wireless links are either based on direct up-conversion of baseband on-off-keying data to the desired RF frequency using electro-optic modulators [10, 11], or up-conversion of a spectral-efficient IF carrier to the RF frequency [12-13]. In the first case, the result is a spectrally inefficient modulation format, and as an example would require atleast 20 GHz of bandwidth to transmit 10 Gb/s data, and in the second case would require complicated electronic arbitrary waveform generator circuits to generate the IF signals. To overcome these challenges, a novel technique for direct generation of advanced modulated wireless signals using baseband data called photonic vector modulation (PVM) has been presented [14, 15]. Photonic vector modulator offers the advantage of simple generation of multi-level quadrature amplitude modulation which offers scalability in both bandwidth and frequency if needed. This work has been performed under the European project

ICT-IPHOBAC [16], where millimeter wave optical devices were designed and fabricated to support the wireless links.

In this report a 16-QAM wireless link generation using photonic vector modulator is presented. Several architectures are proposed, and experimentally demonstrated. In the section II the working principle of the photonic vector modulator is explain. Later, the architectures are described and numerically evaluated. In the section IV a 10 Gb/s 16-QAM wireless signal generation experiment is described, following by conclusion and future work.

II. Working Principle

In a photonic vector modulator, two optical carriers, are modulated with two independent baseband data streams I and Q. The two optical signals can either be of the same source divided into two streams, or two different lasers, and the data modulation can be either direct current modulation of the lasers such as distributed feedback lasers (DFB) or external modulation using electro-optical modulators like Mach-Zehnder modulators (MZM). The two optical signals with the I and Q data modulated, are later modulated with a local oscillator carrier using an external modulator like MZM. The optical signals can be modulated individually or in a combined manner determined by the source of the optical signals. Later, an optical delay of $\Delta\tau = 1/4f_{LO}$ is introduced between the two optical signals, where f_{LO} is the frequency of the LO. This delay corresponds to a 90° phase shift between the I and Q modulated optical signals. When the optical signals are of two different wavelengths λ_1 and λ_2 , this phase shift can be obtained by using a dispersive element like a single mode fibre (SMF) where the length of the fibre is chosen exactly to match the 90° phase shift condition as $\Delta\tau_{21} = D \cdot L \cdot \Delta\lambda_{21}$ where D is the dispersion parameter of the fiber. Figure 2 shows the schematic of a photonic vector modulator.

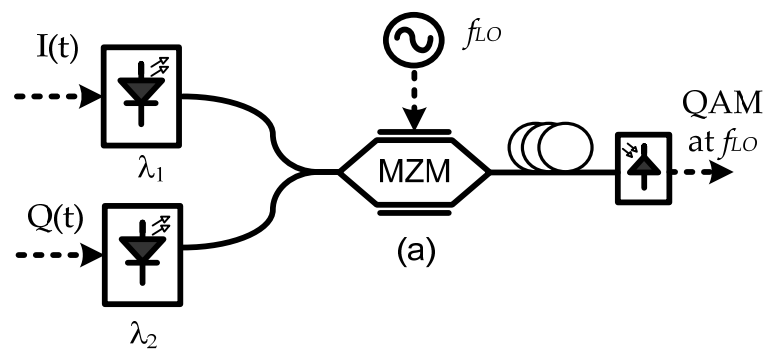


Fig.2. Schematic of a photonic vector modulator.

II.1. Mathematical Model

For the sake of convenience the photonic vector modulator as shown in Fig. 2 is considered. In this schematic two multilevel ($N=4$) baseband signals directly modulate the current of the two DFB lasers. Let the signal $I(t)$ contain the levels $(-A/2, -A/6, A/6, A/2)$. Assuming all the 4 levels have equal probability, the optical power of the laser is given as:

$$P_{avg} = \frac{1}{N} \sum_{n=1}^N P_n,$$

$$P_{n-1} - P_n|_{n=N} = \frac{2\eta A}{N-1} \quad (1)$$

Where η is the internal efficiency of the laser. The dispersion of the fibre is modeled as:

$$H(\Omega) = \frac{1}{\sqrt{L_f}} e^{j\beta(\Omega)} \quad (2)$$

$$\beta(\Omega) = \beta_0 + \beta_1(\Omega - \Omega_0) + \frac{\beta_2}{2}(\Omega - \Omega_0)^2 \quad (3)$$

Where β_1 is the group delay at Ω_0 , and β_2 is related to the dispersion parameter of the fibre as

$$\beta_2 = -\frac{D\lambda_0^2}{2\pi c} \quad (4)$$

Then the LO component at the photodiode output will be

$$i_{pd_LO}(t) = \Re \frac{1}{L_{tot}} J_0(m_{LO}) \cos\left(\frac{\beta_2 L}{2} \omega_{LO}^2\right)$$

$$[[P + \eta I(t)] \cos(\omega_{LO} t) + [P + \eta Q(t - \tau_{21})] \cos(\omega_{LO}(t - \tau_{21}))] \quad (5)$$

where ω_{LO} is the carrier frequency, \Re is the photodiode responsivity, L_{tot} are the optical losses from laser output to photodiode input when the MZM is biased as its maximum transmission point (the 3dB extra due to the MZM Quadrature bias are not considered in this value but in the rest of the equation) and where the MZM model considers only the components at f_{LO} and the higher order harmonics are neglected.

$$m_{LO} = \pi \frac{V_{LO}}{V_\pi} \quad (6)$$

where V_{LO} is the amplitude of the local oscillator tone, and V_π the MZM's half wave voltage. $\Delta\tau_{21} = -\beta_2(\Omega_2 - \Omega_1)$ is the differential delay induced in the optical carriers due to the fibre's chromatic dispersion. When the length of the fibre and the wavelength spacing are chosen to fulfill the quadrature condition as,

$$\Delta\tau_{21} = -\beta_2 L (\Omega_2 - \Omega_1) = \frac{\tau_{LO}}{4} = \frac{1}{4f_{LO}} \quad (7)$$

then the photocurrent is given as,

$$i_{pd_LO}(t) \approx \Re \frac{1}{L_{tot}} J_0(m_{LO}) 2J_1(m_{LO}) \left[[P + \eta I(t)] \cos(\omega_{LO} t) + [P + \eta Q(t) \left(t - \frac{1}{4f_{LO}}\right)] \cos\left(\omega_{LO} t - \frac{\pi}{2}\right) \right] \quad (8)$$

Following the similar procedure, the DC current at the photodetector output is :

$$i_{pd_DC} = \frac{\Re P}{L_{tot}} [J_0^2(m_{LO}) + 2J_1^2(m_{LO})] \quad (9)$$

The noise has its contribution from three sources; the laser relative intensity noise RIN, the photodiode shot noise and the thermal noise from the preamplifier after the photodetector.

$$\sigma_{RIN}^2 = RIN (i_{pd_DC})^2 \Delta f = RIN \left(\frac{\Re P}{L_{tot}} [J_0^2(m_{LO}) + 2J_1^2(m_{LO})] \right)^2 \Delta f \quad (10)$$

$$\begin{aligned} \sigma_{shot}^2 &= 2q (i_{pd_DC} + i_{dark}) \Delta f \\ &= 2q \left(\frac{\Re P}{L_{tot}} [J_0^2(m_{LO}) + 2J_1^2(m_{LO})] + i_{dark} \right) \Delta f \quad (11) \end{aligned}$$

$$\sigma_{thermal}^2 = \frac{4kT\Delta f}{R_L} F \quad (12)$$

Where R_L is the load resistance, and F is the noise figure of the preamplifier. From the above noise components, the SNR of the signal is expressed as:

$$\frac{S}{N} = \frac{P_{pd_data}}{\sigma_{RIN}^2 R_L + \sigma_{shot}^2 R_L + \sigma_{thermal}^2 R_L} = \frac{1}{\Delta f (N-1)^2} \frac{(2\Re J_0^2(m_{LO}) J_1^2(m_{LO}))^2 \eta^2 A_{peak}^2}{RIN \left(\Re P [J_0^2(m_{LO}) + 2J_1^2(m_{LO})] \right)^2 + 2q \left(\Re P [J_0^2(m_{LO}) + 2J_1^2(m_{LO})] + i_{dark} \right) + \frac{L_{tot} 4kTF}{R_L}} \quad (12)$$

where N is the level of modulation ($N=2$ for QPSK, $N=4$ for 16-QAM). From the equation 12 it is clear that by increasing the number of levels the SNR of the signal changes drastically. But on the other hand the SNR can be improved by increasing the modulation extinction ratio of the optical signal either by incorporating high ER lasers, or external modulators which have around 10 dB more ER than directly modulated lasers. From the expression 12 it can be concluded that 16-QAM has 4.5 times lower SNR compared to QPSK.

The general behaviour of the PVM system for a QPSK modulation is shown in Fig. 3, which contains the variation of SNR w.r.t the modulation index of the LO at different laser RIN.

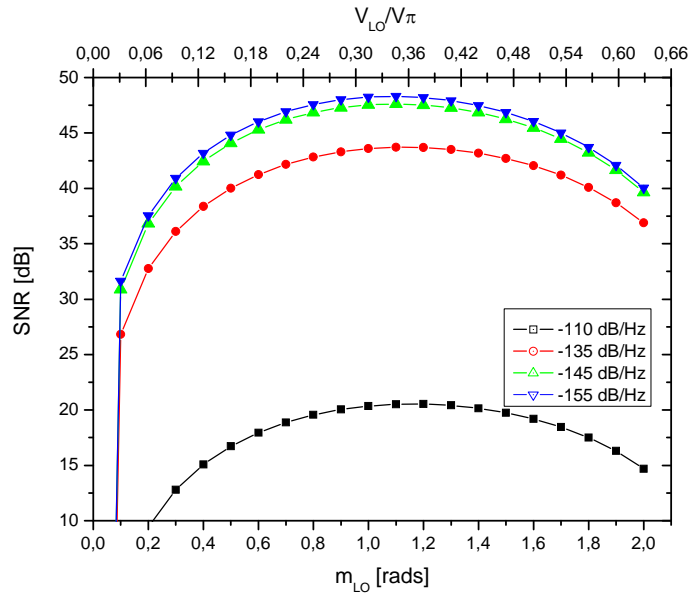


Fig.3. SNR vs m_{LO} plotted against various laser RIN values.

III. Experimental Demonstrations

In this section, various experimental demonstrations of 16-QAM wireless signal generation is presented. First a 16-QAM link based on direct modulated lasers, and dispersive element as shown in Fig. 2 is presented, and later the use of external modulators and optical delay line in photonic vector modulator for 16-QAM generation is presented.

III.1. Architecture 1: Direct modulation based PVM

The architecture is as shown in Fig. 2. Two DFB lasers emitting at 1550.92 nm and 1459.026 nm with 1 GHz modulation bandwidth were used in order to generate a 2.5 Gb/s 16-QAM signal at a carrier frequency of 42 GHz. Two 625 Mbaud 4ASK (amplitude shift keyed) were generated using an arbitrary waveform generator. The 1.25 Gb/s 4ASK signals with 2Vpp directly modulate the two DFB lasers. The two optical signals were combined using a 3-dB coupler and modulated by a +15 dBm 42 GHz carrier using a 45 GHz bandwidth MZ modulator. Later, an optical fibre of length 340 m with dispersion coefficient of 16.5 ps/km.nm was used to induce a delay corresponding to 90° phase shift between the LO signals modulated on the two optical carriers. The output of the SMF is fed into a photodetector, whose output is a 2.5 Gb/s 16-QAM wireless signal at 42 GHz carrier. Fig. 4 shows the RF spectrum of the wireless signal.

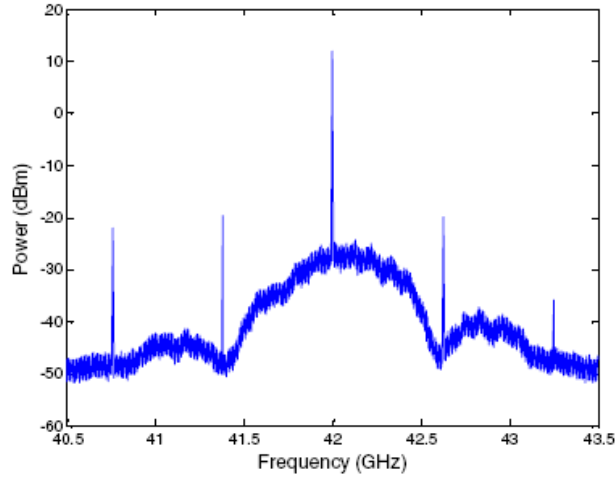


Fig. 4. Electrical spectrum of a 2.5 Gb/s 16-QAM signal at 42 GHz bandwidth.

From the fig. 4 it can be seen that a huge unwanted LO signal is present which will limit the amplifiers in the link. To avoid this, a third unmodulated laser following the condition $\Delta\tau_{31} = 2.5\Delta\tau_{21}$ and $P_3 = \sqrt{2}P$, where P is the average power of both the modulated lasers. By following this conditions, a situation arises where the LO component cancels and a resulting spectrum as shown in Fig. 5 is obtained.

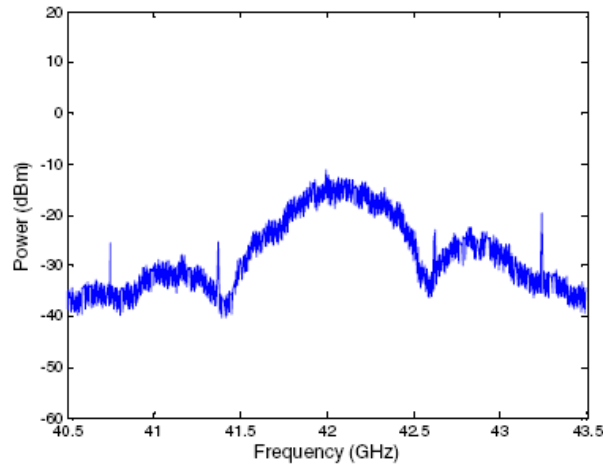


Fig. 5. Electrical spectrum of a 2.5 Gb/s 16-QAM signal at 42 GHz bandwidth, with the third unmodulated laser.

To demodulate the wireless signals, the generated signals were mixed with another copy of the LO in a 42 GHz mixer, and by changing the phase of the LO signal the I and Q data are demodulated one at a time. Figure 6a, shows the inphase and quadrature demodulated 4ASK signals respectively. From the statistical data of the eye diagrams, the error vector magnitude of the signal was calculated as -17.83 dB. Figure 6b shows the constellation diagram of the demodulated 16-QAM signal.

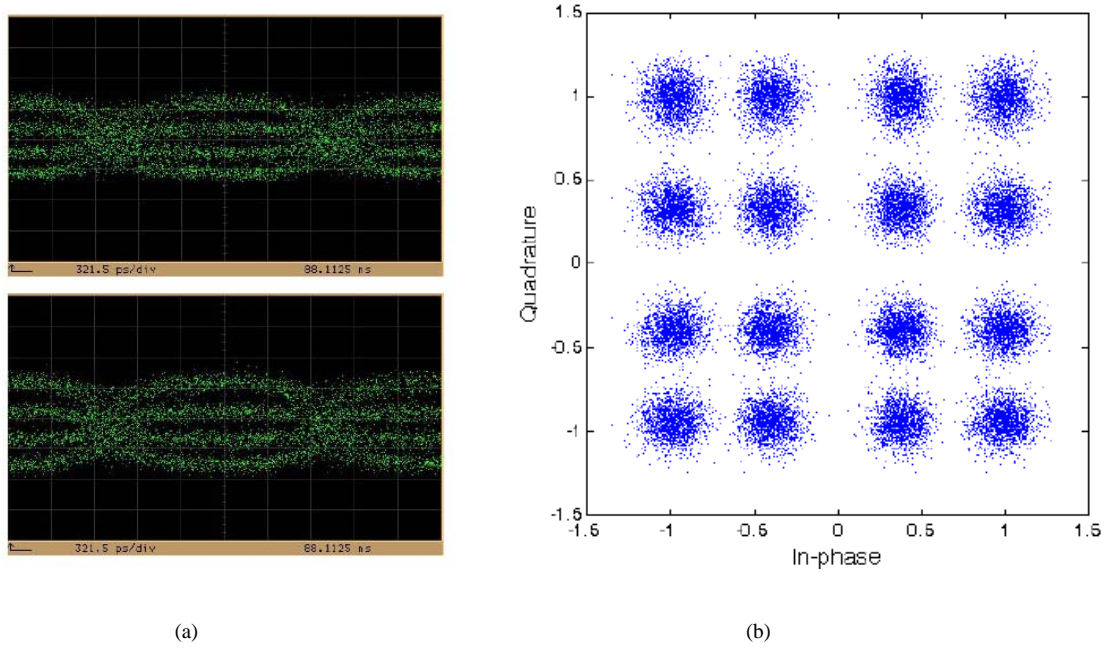


Fig. 6. The inphase (top) and quadrature demodulated eye diagrams(a), the constellation diagram obtained from the eye diagrams (b).

I.1. Architecture 2: DD-MZM based PVM

Figure 7 shows the schematic of the proposed PVM approach. The outputs of two continuous wave (CW) lasers are launched into two DD-MZMs. Each arm of the DD-MZM is independently driven by baseband data (I_1 , I_2 and Q_1 , Q_2) where the voltage applied to one arm is twice that of the one applied to the other for generating an optical 4ASK signal, i.e. $I_2=I_1/2$ V and $Q_2=Q_1/2$ V. The two 4ASK baseband optical signals are modulated by a 40 GHz LO signal using two MZM modulators. Later the quadrature arm is optically delayed by $\Delta T=1/4f_{LO}$ using a tuneable ODL. The combined output, shown in Fig. 2a is photodetected resulting in a 16QAM modulated mm-wave carrier at f_{LO} .

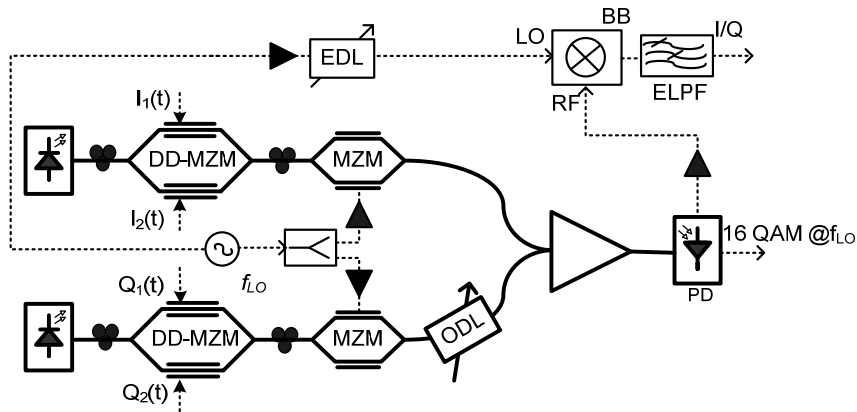


Fig. 7. Experimental setup of the DD-MZM based PVM.

The arrangement shown in Fig. 7 was set-up in the laboratory to demonstrate the proposed generation technique. To analyse the quality of the transmitter, the signals were demodulated using a typical electrical receiver and the EVM calculated from the demodulated I and Q eye diagrams. To calculate the EVM from the captured eye diagrams, the histogram of each level was plotted, and μ (mean) and σ (standard deviation) were measured. Later, a Gaussian distribution of each symbol was generated using the extracted μ and σ , and normalised. The resulting measured symbols were compared with the ideal values of 16QAM (1, 1/3, -1/3, -1) and the EVM computed. This procedure was followed for both PVM architectures.

CW light from two DFB lasers at wavelengths 1548.5 nm and 1550.4 nm with +10 dBm optical power are launched into two DD-MZMs biased at the quadrature bias point. Two electrical baseband data of 2.2 Gb/s at 1 V and 0.45 V are used to drive the two arms of the DD-MZM, resulting in a 4.4 Gb/s optical baseband 4ASK signal, as shown in Fig. 8b and 8c. Electrical low pass filters with a 3-dB cut-off of 1.65 GHz were used. Because of the unavailability of filters with higher cut-off the baseband data was limited to 2.2 Gb/s. The two optical 4ASK signals are later modulated with a +15 dBm 40 GHz mm-wave carrier using two different MZMs. The lower arm is optically delayed by $T=1/4f_{LO}$, in order to generate the 90° phase shift between the two mm-wave carriers that grants the quadrature condition. The two mm-wave modulated signals are combined and amplified up to +5 dBm using an EDFA and photo detected resulting in a 16QAM modulated carrier at 40 GHz.

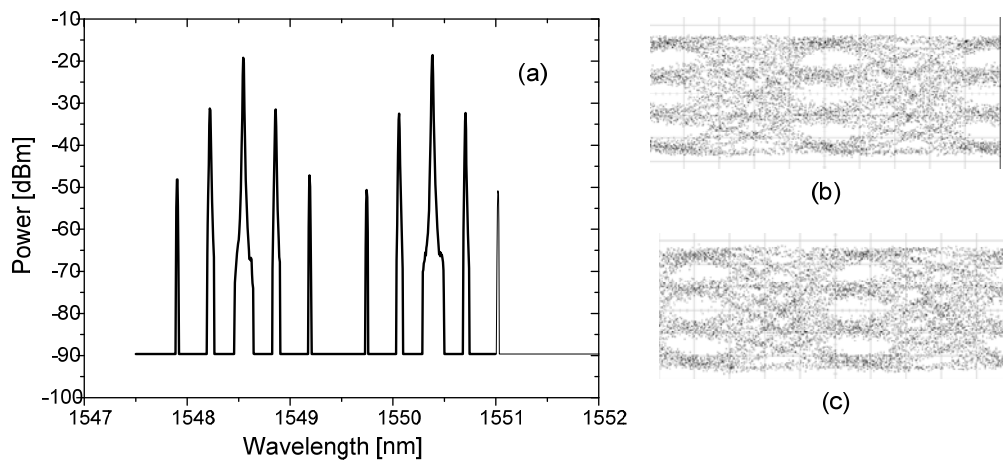


Fig. 8. The optical spectrum before the photo diode in schematic 1(a), the Inphase (b) and Quadrature (c) eye diagrams output at the DD-MZM.

First, experiments were performed in order to generate 2 and 4 Gb/s 16-QAM modulated 40 GHz carriers using this PVM architecture. The down converted I and Q eye diagrams were captured using an 80 GHz oscilloscope. Fig. 9 shows the eye diagrams and the normalised constellation of the downconverted 8.8 Gb/s 16QAM signal components.

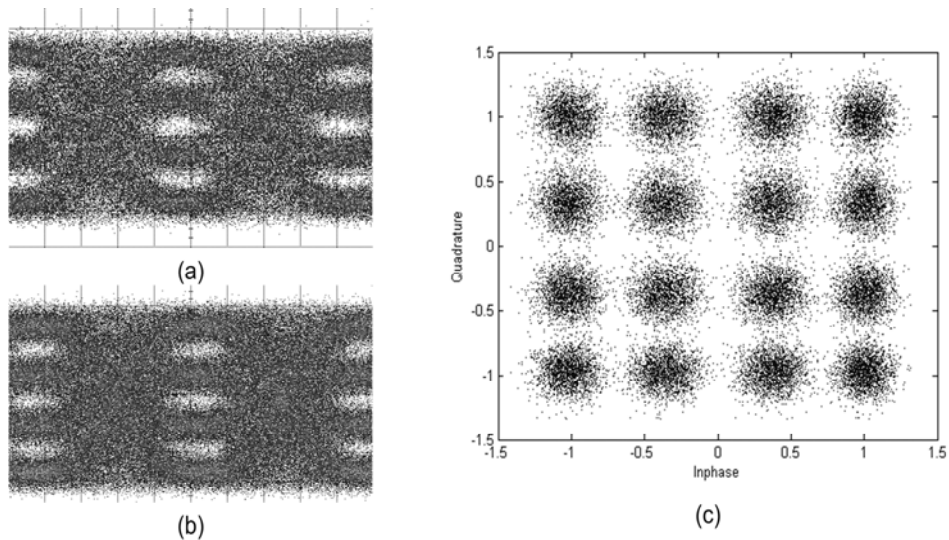


Fig. 9. Downconverted 8.8 Gb/s In-phase (a), and Quadrature (b) components, and resulting normalised constellation diagram(c).

Table 2: EVM calculated at different data rates.

Bit Rate (Gb/s)	EVM (dB)
2	-17.23
4	-16.41
8.8	-15.77

Table 2: EVM of the 16-QAM signals calculated at different bit rates.

The EVM of the 16QAM modulated carriers is presented in the table 2. The measured EVM increases with the bit rate because of the limited bandwidth of the electronic components (filters, mixer and amplifier) available in the laboratory.

IV. 10 Gb/s 16-QAM Signal Generation

In this photonic vector modulation scheme, a single continuous wave optical source is modulated with an mm-wave carrier using a Mach-Zehnder modulator biased at the quadrature bias (QB) point. The mm-wave carrier modulated optical signal is split in two arms: I and Q using a 3-dB power splitter. To induce a 90° phase shift between the I and Q mm-wave carriers, the Q arm optical signal is delayed by $\Delta T = 1/4f_{LO}$ using a tunable optical delay line. This optical delay between the I and Q arm optical induces a 90° phase shift between the photo detected electrical carriers. Two DD-MZMs are used in each arm for modulating baseband data. Both modulators are biased at QB for generating amplitude modulation, the upper modulator is driven with two

independent data $I_1(t)$ and $I_2(t)$, and the lower with data $Q_1(t)$ and $Q_2(t)$ where the amplitudes follow the condition $I_2 = I_1/2$ V, and $Q_2=Q_1/2$ V for generating four amplitude levels resulting in 4ASK signals in each arm. Fig. 1 shows the schematic of the PVM architecture. The upper arm (I) and the lower arm (Q) are photo mixed and combined in a balanced photodetector (BPD). The electrical output of the photodetector is a 16QAM modulated mm-wave carrier.

Equation 13 represents the resulting photo current.

$$i_{PD} = \frac{\Re P}{L_{tot}} J_0(m_{LO}) J_1(m_{LO}) \left[\begin{array}{l} \cos^2\left(\frac{\pi}{4V_\pi} I_1(I_1(t) - I_2(t))\right) \cos(\omega_{LO}t) \\ + \cos^2\left(\frac{\pi}{4V_\pi} Q_1(Q_1(t) - Q_2(t))\right) \sin(\omega_{LO}t) \end{array} \right] \quad (13)$$

Where R is the responsivity of the photodetector, P the output power of the laser, L_{tot} the total insertion losses, $m_{LO}=\pi V_{LO}/V_\pi$, and J_n the Bessel function of nth order.

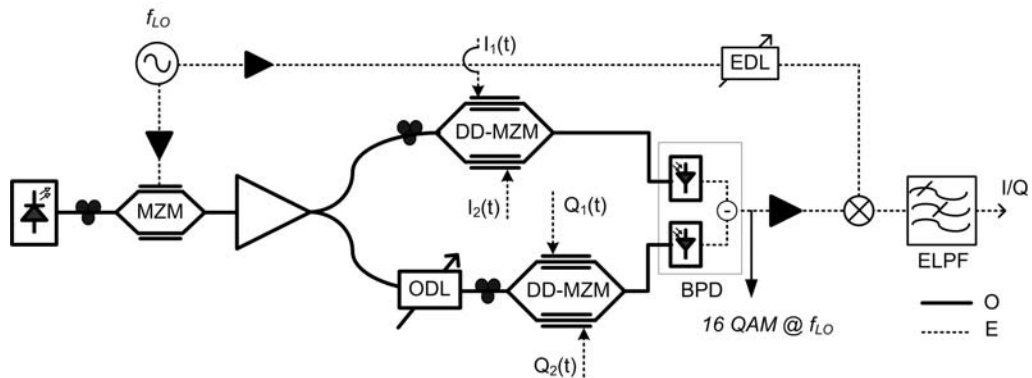


Fig.10. Schematic of the proposed 16QAM photonic vector modulator architecture.

IV.1. Experimental Results

Figure 10 shows the schematic of the photonic vector modulator. A continuous wave DFB laser at 1555.4 nm with an output power of +15 dBm is externally modulated by a 42 GHz local oscillator carrier using a 50 GHz MZM biased at the QB point. The output of the MZM is amplified to +18 dBm using an EDFA to compensate the 6 dB insertion losses of the modulator, and the 3 dB losses due to QB. The output of the EDFA is divided into two arms using a 3 dB splitter: upper (I) and lower (Q). The Q-arm optical signal is delayed using an ODL to generate a 90° phase shift between the I and Q modulated LO carrier components. The I and Q optical components were corrected for polarization mismatch using a polarization controller. Two 40 GHz DD-MZMs biased at QB were used for generating the I and Q 4ASK signals. The two arms of the I-DD-MZM are driven with two 2.5 Gbit/s independent data I_1 and I_2 where I_1 was tuned to 1 V pp and I_2 to 0.5 V pp, resulting in 5 Gbit/s 4ASK modulation. Similarly the Q-arm DD-MZM was driven by 2.5 Gbit/s Q_1 and Q_2 data resulting in another 5 Gbit/s 4ASK. The I and Q optical signals with both the baseband data and RF signal modulated on them were photodetected and added in a

45 GHz BPD with 0.53 A/W responsivity. The output of the BPD is a 10 Gbit/s 16QAM modulated 42 GHz carrier. Fig. 11 shows the RF spectrum of the generated 16QAM 42 GHz carrier.

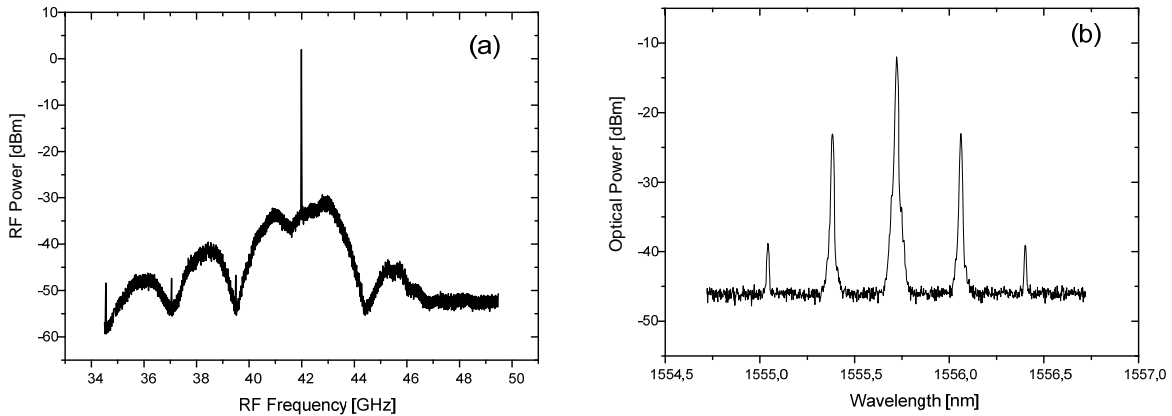


Fig. 11. The RF spectrum at the output of the balanced photodetector (a), and the optical spectrum at the output of the MZ modulator(b).

To analyse the quality of the generated, the 16QAM signal was demodulated using an electrical mixer. The 16QAM signal output at the balanced photodetector was amplified and input to a 42 GHz broadband electrical mixer, and mixed with the same LO used at the transmitter. The baseband output of the electrical mixer was filtered using an electrical low pass filter with a 3-dB cut-off frequency of 1.87 GHz. The I and Q components of the 16QAM signal were demodulated electrically by tuning the phase of the LO carrier input to the mixer using a tunable electrical delay. When the electrical delay was tuned to have 0° phase between the LO and the received 16QAM carriers, I signal was demodulated, and for 90° , the Q signal.

IV.2. Results

Figure 12 (a) and (b) show the demodulated *I* and *Q* eye diagrams of the 10 Gbit/s 16QAM mm-wave carriers generated by the above described PVM configuration. To analyze the quality of the received signal EVM is calculated from the statistical data of the eye diagrams. To calculate the EVM from the captured 4ASK *I* and *Q* eye diagrams, the histogram of each level was plotted and the mean μ , and the standard deviation σ were measured. Later a Gaussian distribution of each symbol was generated using the μ and σ and normalized to 1. The resulting symbols from the Gaussian distribution were compared with the ideal values for 16QAM (1, 1/3, -1/3, -1) and the EVM computed. It should be noted that the EVM of the signal is calculated after the receiver stage, and an ideal receiver would improve the EVM. The EVM of the 10 Gbit/s 16QAM modulated 42 GHz carrier was calculated to be -18.33 dB. The EVM calculated does not totally reflect the quality of the PVM but contains contribution from the electrical demodulation which incorporates bandwidth limited components. For e.g., the mixer and the amplifiers have an electric bandwidth of

around 3 GHz. Also, the photodetector used in the PVM has an uneven response at 41 GHz, which can be noted from the figure 2. The EVM can be improved by accurate phase matching at the electrical receiver by using a phase locking mechanism. To prove this claim, instead of vectorial 16QAM modulated, 5 Gbit/s 4ASK modulation was performed (5 Gbit/s 4ASK and 10 Gbit/s 16QAM have the same electrical bandwidth: 5 GHz) with only one DD-MZM and at the same LO frequency, 42 GHz. The generated 4ASK signal's EVM was calculated to be -21.04 dB, which is a 3 dB improvement at the same electrical bandwidth.

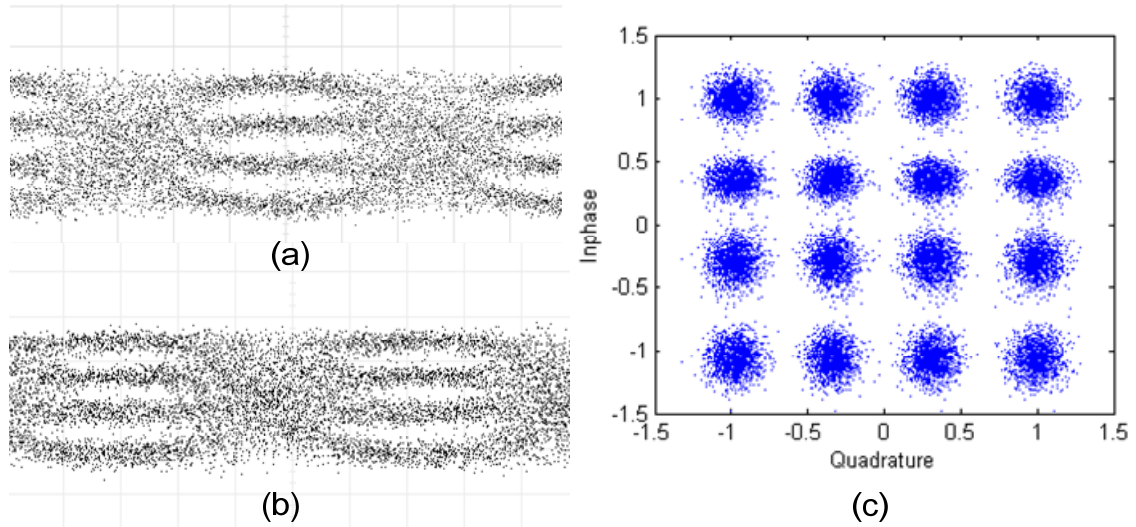


Fig.12. The inphase (a), and the quadrature (b) demodulated eye diagrams, and the resulting constellation (c) of a 10 Gb/s 42 GHz 16-QAM signal.

V. Conclusions

In this master thesis the application of photonic vector modulation for generation of 16-QAM signals is presented. The photonic vector modulation technique proves to be a good candidate for providing high capacity millimeter-wave wireless links. The main advantages of this technique are that it is scalable in both frequency and bit-rate which enables this technology to be future proof. According to the requirements and the cost, various architectures can be designed based on either cheap low bandwidth directly modulated lasers, or high performance external modulators. The main parameter that enables the generation of 16-QAM modulation is the extinction ratio of the baseband modulation, where higher extinction ratios are desired. Using this technique successful demonstration of a 10 Gb/s 16-QAM wireless signal generation at 42 GHz is presented.

AGRADECIMIENTOS

This work has been carried out under the FP6 European Project ICT-IPHOBAC, and NoE ISIS.

BIBLIOGRAFÍA

- [1] A. H. Gnauck, and P. Winzer, "Optical Phase-shift-keyed transmission," *J. Lightwave Technol.*, vol. 23, no. 1, pp. 115-130, 2005.
- [2] A. H. Gnauck, P. J. Winzer, S. Chandrasekhar, and C. Dorrer, "Spectrally efficient (0.8 b/s/Hz) 1-Tb/s (25 x 42.7 Gb/s) RZ-DQPSK transmission over 28 100-km SSMF spans with 7 optical add/drops," in *Proc. Optical Fiber Communication Conf., OFC 2004*, Paper Th4.4.1, 2004.
- [3] D. Van den borne, S. L. Jansen, E. Gottwald, E. D. Schmidt, G. D. Khoe, and H. de Waardt "DQPSK modulation for robust optical transmission," in *Proc. Optical Fiber Communications Conf., OFC 2008*, paper OMQ1, 2008.
- [4] H. C. Hansen Mulvad, M. Galili, L. K. Oxenlowe, H. Hu, A. T. Clausen, J. B. Jensen, C. Peucheret, and P. Jeppesen, "Error-free 5.1 Tb/s data generation on a single-wavelength channel using a 1.28 Tbaud symbol rate," in *Proc. Annual meeting of the IEEE Photonics Society 2009*, paper PD 1.2, 2009.
- [5] <http://www.ieee802.org/3/av/>
- [6] D. Qian, N. Cvijetic, J. Hu, and T. Wang, "40-Gb/s MIMO-OFDM-PON using polarization multiplexing and direct-detection," in *Proc. Optical Fiber Communications Conf., OFC 2009*, paper OMV3, 2009.
- [7] D. Qian, N. Cvijetic, J. Hu, and T. Wang, "108 Gb/s OFDMA-PON with polarization multiplexing and direct detection," *J. Lightwave Technol.*, vol. 28, no. 4, pp. 484-493, 2010.
- [8] A. J. Seeds and K. J. Williams, "Microwave photonics," *J. Lightwave Technol.*, vol. 24, no.12, 4628–4641 2006.
- [9] J. Capmany and D. Novak, "Microwave photonics combines two worlds," *Nature Photon.* 1,319–330 2007.
- [10] A. Hirata, M. Harada, and T. Nagatsuma, "120-GHz wireless link using photonic techniques for generation, modulation, and emission of millimeter-wave signals," *J. Lightwave Technol.*, vol. 21, no. 10, pp 2145-2153, 2003.
- [11] R. W. Ridgway, and D. W. Nippa, "Generation and modulation of a 94-GHz signal using electrooptic modulators," *Photonics Technol. Lett.*, vol. 20, no.8, pp. 653-655, 2008.
- [12] C.-T. Lin, E.-Z. Wong, W.-J. Jiang, P.-T. Shin, J. Chen, and S. Chi "28-Gb/s 16-QAM OFDM radio-over-fiber system within 7-GHz license-free band at 60 GHz employing all-optical up-conversion," *Lasers and Electro-Optics, 2009 and 2009 Conference on Quantum electronics and Laser Science Conference. CLEO/QELS 2009*.
- [13] M. Weiss, A. Stoehr, F. Lecoche, B. Charbonnier, 27 Gbit/s Photonic Wireless 60 GHz Transmission System using 16-QAM OFDM, *International Topical Meeting on Microwave Photonics, MWP 2009*, Oct. 14-16, Valencia, Spain, 2009, (post deadline paper).

- [14] R. Sambaraju, M. A. Piqueras, V. Polo, J. L. Corral, and J. Martí, "Generation of multi-gigabit-per-second MQAM/MPSK-modulated millimeter-wave carriers employing photonic vector modulator techniques," *J. Lightwave Technol.*, vol. 25, no. 11, pp. 3350-3357, 2007.
- [15] R. Sambaraju, J. L. Corral, V. Polo, J. Martí, "Ten gigabits per second 16-level quadrature amplitude modulated millimeter-wave carrier generation using dual-drive Mach-Zehnder modulators incorporated photonic vector modulator," *Optics Letters*, vol. 33, no. 16, pp. 1833-1835, 2008.
- [16] IPHOBAC: www.ist-iphobac.org

ANEXO

- a) Rakesh Sambaraju, Miguel Ángel Piqueras, Valentin Polo, Juan Luis Corral, and Javier Marti, "Photonic vector modulation of 3.6 Gb/s 16QAM at 39 GHz for radio-on-fibre systems," in Proc. European Conference on Optical Communications 2007, ECOC 2007, Tu. 5.4.7, Berlin, September 2007.
- b) Rakesh Sambaraju, Valentin Polo, Juan Luis Corral and Javier Marti, "16-QAM 10 Gb/s mm-wave wireless links employing photonic vector modulation techniques," in ICT Mobile Summit, Stockholm, June 2008.
- c) Rakesh Sambaraju, Valentin Polo, Juan Luis Corral and Javier Marti, "Ten gigabits per second 16-level quadrature amplitude modulated millimeter-wave carrier generation using dual-drive Mach-Zehnder modulator incorporated photonic vector modulator," *Optics Letters*, vol. 33, no. 16, pp. 1833-1835, 2008.
- d) Juan Luis Corral, Rakesh Sambaraju, Miguel Ángel Piqueras, and Valentin Polo, "Pure 2.5 Gb/s 16-QAM signal generation with photonic vector modulator," *IEEE/MTTS International Microwave Symposium Digest 2008*, IMS paper We4D-03, Jun. 2008.